Available online at www.sciencedirect.com

ScienceDirect

Geochimica et Cosmochimica Acta 242 (2018) 21–33

Geochimica et Cosmochimica Acta

www.elsevier.com/locate/gca

Using deuterium excess, precipitation and runoff data to determine evaporation and transpiration: A case study from the Shawan Test Site, Puding, Guizhou, China

Yundi Hu [a,b,c], Zaihua Liu [a,b,*], Min Zhao [a,b], Qingrui Zeng [a,b,c], Cheng Zeng [a,b], Bo Chen [d], Chongying Chen [a,c], Haibo He [a,c], Xianli Cai [a,b,c], Yi Ou [b], Jia Chen [b]

[a] *State Key Laboratory of Environmental Geochemistry, Institute of Geochemistry, CAS, Guiyang 550081, Guizhou, China*

[b] *Puding Karst Ecosystem Research Station, Chinese Ecosystem Research Network, Chinese Academy of Sciences, Puding 562100, Guizhou, China*

[c] *University of Chinese Academy of Sciences, Beijing 100049, China*

[d] *Institute of Public Administration, Guizhou University of Finance and Economics, Guiyang 550025, Guizhou, China*

Received 19 January 2018; accepted in revised form 30 August 2018; available online 14 September 2018

Abstract

Separating watershed evapotranspiration into its evaporation and transpiration components is important for calculating the carbon that is assimilated by terrestrial vegetation in carbon cycle studies. The key step in this separation is to quantify the evaporation component. The deuterium excess (d-excess) in meteoric water has been shown to be an important indicator of both the original source of the water vapor and the humidity at the vapor source area. It has also shown promise for use in investigating the evaporation losses. While many studies have used the $\delta D/\delta^{18}O$ method to study watershed evaporation, few have discussed the differences between the $\delta D/\delta^{18}O$ (single isotope system) and d-excess (dual isotope system) methods in quantifying watershed evaporation. Given the complexity of natural watersheds, the Shawan Test Site was established at Puding, China, to study the water cycle in five concrete tanks (simulated watersheds) with different land uses over one hydrologic year. There were no plants in two of the tanks (bare rock and bare soil), which allowed verification of evaporation calculations derived from the d-excess and $\delta D/\delta^{18}O$ methods. δD or $\delta^{18}O$ values of precipitation in the rainy season, when most of the groundwater recharge occurs, showed great variability. In contrast, the d-excess of the meteoric waters collected during the same rainy season was much more stable than the δD or $\delta^{18}O$ values. We quantified the annual evaporative loss of the five watersheds using both methods. Comparison of the results indicated that the d-excess method is more acceptable than the $\delta D/\delta^{18}O$ method due to the stability of d-excess. Calculated ratios of transpiration to evapotranspiration in three tanks planted with vegetation were 56.8% in cultivated land, 70.9% in shrub land, and 85.9% in grassland, demonstrating that in well vegetated watersheds, this component of the cycle is controlled chiefly by plant transpiration. Land use has an important impact on the hydrologic cycle in a watershed, and the d-excess calculations conducted in this study provide new insights for quantifying components of the cycle, especially in the East Asian monsoon region which has rainfall with a large range in δD or $\delta^{18}O$ values.

Keywords: Deuterium excess; Stable water isotopes; Land use type; Plant transpiration; Watershed evaporation; Water cycle

* Corresponding author at: State Key Laboratory of Environmental Geochemistry, Institute of Geochemistry, CAS, Guiyang 550081, Guizhou, China.

E-mail address: liuzaihua@vip.gyig.ac.cn (Z. Liu).

https://doi.org/10.1016/j.gca.2018.08.049

0016-7037/

1. INTRODUCTION

On land, water returns to the atmosphere through transpiration by plants, a process which does not involve isotopic fractionation during uptake (Wershaw et al., 1966; Ehleringer and Dawson, 1992), or through evaporation from water and soil that does involve fractionation. Knowledge of the transpiration and runoff in watersheds provides a first-order evaluation of the biological uptake of CO_2 (Beer et al., 2007; Liu et al., 2010). Several studies have noted the significance of water and carbon fluxes in the Earth's terrestrial system (Ferguson and Veizer, 2007; Wang and Dickinson, 2012), so it is of considerable importance to partition the water cycle within watersheds. However, it is difficult to quantify the aqueous fluxes in a cycle, and especially difficult to separate evapotranspiration into its evaporation and transpiration components. Recent studies have provided evidence that transpiration far exceeds physical evaporation on the continents (with the exception of Antarctica presumably) as a whole, but the precise proportions attributable to the two processes continues to be refined (Jasechko et al., 2013; Sutanto et al., 2014; Maxwell and Condon, 2016). Studies of global evapotranspiration have mainly been conducted in arid and semi-arid areas. In China, many studies have been conducted in arid areas such as the North and Northwest, but few have focused on the southern and southwestern regions that are humid and have dense vegetation (Schlesinger and Jasechko, 2014). In addition, most previous studies were conducted only at the pilot scale and very few have attempted to separate the evaporation and transpiration components at the watershed scale (Sulman et al., 2016).

Recent studies have shown that the partition of evapotranspiration can be estimated in three ways: by field measurement, applying land surface models, or aqueous isotope studies (Sutanto et al., 2014). Field measurements will be accurate at a given test site but it is difficult to extrapolate their data to calculate the evaporation from large bodies of soil and water or the transpiration from vegetation at the watershed scale. When using a land surface model it is more difficult to partition watershed evapotranspiration because this will require extensive monitoring networks to provide the substantial data base needed to calibrate and validate the areal model. Alternatively, we can separate watershed evapotranspiration into the evaporation and transpiration components using hydrogen and oxygen, the stable isotopes of water. In previous studies, evaporation in a watershed has been calculated by comparing the difference between the initial isotopic composition of the groundwater with the final composition at a watershed outlet (Gonfiantini, 1986; Gibson et al., 1993; Telmer and Veizer, 2000; Lee and Veizer, 2003; Ferguson and Veizer, 2007). This method usually obtained evaporation estimates on the timescale of hydrological year, given the groundwater residence times in the majority of watersheds (Lee and Veizer, 2003). Discrepancies between the three methods remain, but it has been shown that field measurement and isotope-based methods are consistent with each other within their error margins, whereas models tend to produce higher estimates of evaporation (Sutanto et al., 2014; Schlesinger and Jasechko, 2014). Therefore, stable isotopes play an important role in quantifying the partition of evapotranspiration. Furthermore, the d-excess (d-excess = $\delta D - 8\delta^{18}O$, as defined by Dansgaard (1964)), has shown promise for investigating evaporation, although it can be an indicator of both the original source of the water vapor and of relative humidity conditions in that source area (Araguas-Araguas et al., 1998; Masson-Delmotte et al., 2005). Several studies have estimated the evaporation in watersheds using d-excess (Machavaram and Krishnamurthy, 1995; Huang and Pang, 2012), but few have systematically explained the mechanisms underlying the factors that influence d-excess, or compared the differences between d-excess and $\delta D/\delta^{18}O$ in estimating watershed evaporation. In this study, we have estimated the evaporation in five simulated watersheds using both methods, demonstrating that the δD and/or $\delta^{18}O$ of precipitation may display great variability (thus impacting the reliability of calculations of evaporation) but the d-excess of meteoric water is much more stable. Therefore, application of the d-excess method revealed in this article provides new insight for quantifying a watershed hydrologic cycle.

2. THE STUDY SITE

The simulated test site (26°14′–26°15′N, 105°42′–105°43′E, 1200 m) is located in the Puding Comprehensive Karst Research and Experimental Station, Guizhou Province, China (Fig. 1a). The climate is humid, subtropical monsoonal, with an annual average air temperature of ~15.1 °C, average annual precipitation of 1315 mm, about 80% of which occurs during the rainy season from May to October (Yang et al., 2012), and average annual relative humidity of 78% (China Meteorological Data Network, China Meteorological Administration). The test site consists of five adjoining concrete tanks made up to simulate five different types of land use: bare rock, bare soil, cultivated soil, grassland, and shrub land (Fig. 1b): details can be found in Zeng and Liu (2013), Chen et al. (2017) and Zeng et al. (2017). Each tank is 20 m long, 5 m wide and 3 m deep. The tanks are coated with epoxy resin, which acts as an aquiclude to prevent groundwater leakage. Each tank is filled with 2.5 m of dolomitic limestone rubble topped with 0.5 m of calcareous soil, with the exception of the bare rocky model which is filled only with the rubble and has no plants. The 2.5 m dolomitic limestone rubble and 0.5 m soil are identical in all tanks. The bare soil land has no plants but has soil and carbonate rubble. The cultivated tank was planted with corn, whose growing season is from May to August. Alfalfa and Roxburgh roses were sown into the soils of the grassland and shrub land respectively in January 2014. There is a drainage outlet hole in each tank to simulate a karst spring, plus a measuring device to monitor water level change (Fig. 1c). Since each tank functions as a small but a complete watershed, we term them "simulated watersheds" in the following text.

3. METHODS

3.1. Sampling and analysis

From November 2015 to November 2016 at the study site, rainfall samples were collected by standard gauges

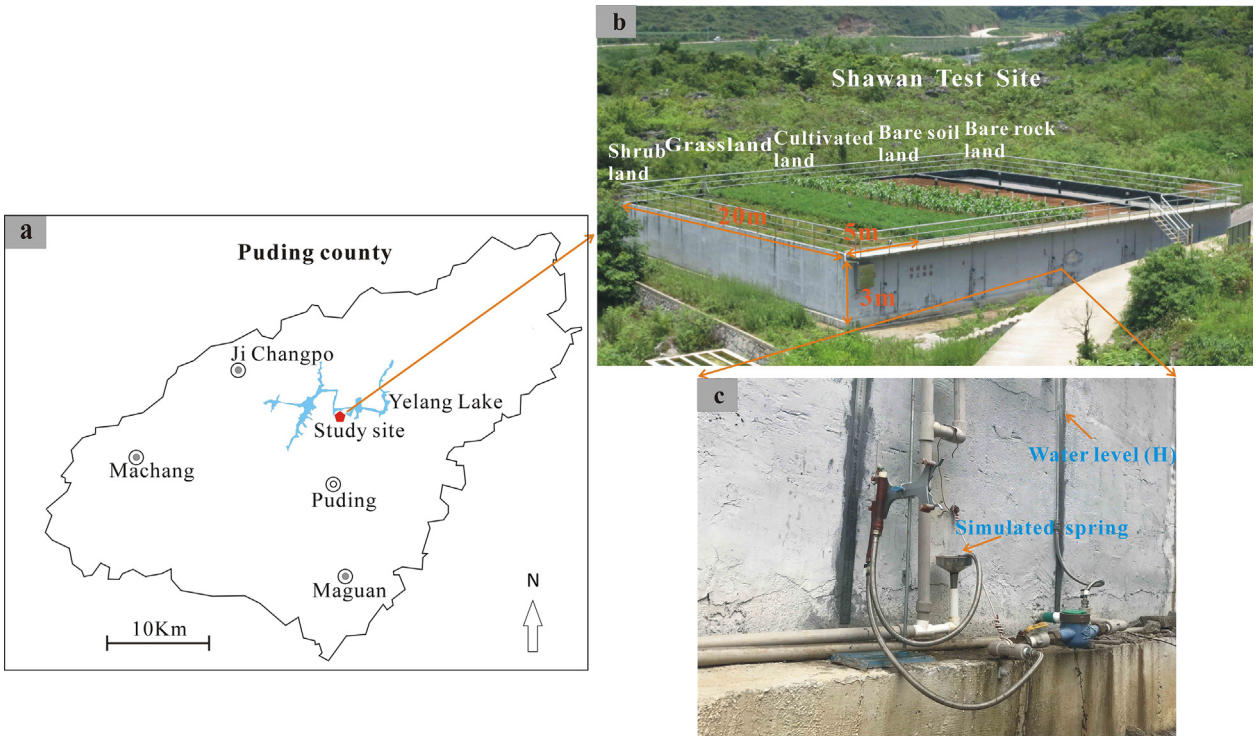

Fig. 1. (a) The location of the study site in Puding County, Guizhou Province. (b) The Shawan Test Site consists of five concrete tanks that simulate watersheds with different land uses: bare rock (coarse gravel) land, bare soil land, cultivated land (corn), grassland (alfalfa), and shrub land (Roxburgh roses). (c) The photo shows the device used to measure water level and groundwater discharge.

and passed through 0.45 μm Millipore filters into 20 ml high-density polyethylene bottles immediately after each rainfall event. The total number of samples (events) was 105. Groundwater samples were also passed through 0.45 μm Millipore filters into 20 ml high-density polyethylene bottles. To obtain high resolution isotopic compositions, each groundwater outlet was sampled at a 10-day interval, with the discharge and water level data being measured during sampling. All of the samples were sealed with Parafilm and stored in a refrigerator at ~4 °C. δD and $\delta^{18}O$ of the precipitation and groundwater samples were determined using a Los Gatos Research DLT-100 liquid isotope water analyzer at the State Key Laboratory of Environmental Geochemistry, Institute of Geochemistry, Chinese Academy of Sciences, using the methods described in Lis et al. (2008). The standards, purchased from Los Gatos Research Inc. as well, have four different isotopic compositions (δD, $\delta^{18}O$): (−123.6‰, −16.1‰) for LGR2A, (−96.4‰, −13.1‰) for LGR3A, (−51.0‰, −7.7‰) for LGR4A, and (−9.5‰, −2.8‰) for LGR5A. We selected the three appropriate standards from them to encompass the isotopic compositions measured in the samples. The standard deviation (1σ) of measurement performed was ±0.5‰ for δD and ±0.1‰ for $\delta^{18}O$. All standards and measured values are reported relative to Vienna-Standard Mean Ocean Water (VSMOW).

3.2. Theoretical background

Precipitation undergoes a series of processes, e.g., evaporation and transpiration, from the time it lands as stem flow on any plants and/or infiltrates the surface to recharge the groundwater. Thus, the processes that precipitation underwent in the watershed are recorded in the groundwater, and it is reasonable to study these processes by investigating the groundwater isotopic characteristics. In this study, evaporation from the soil surface is estimated from the d-excess and $\delta^{18}O$ or δD resulting from the associated fractionation. In addition, by combining the evaporation estimated by the d-excess and $\delta^{18}O$/δD methods with the actual evapotranspiration calculated from the water balance, the transpiration losses can be estimated, including interception by plants.

3.2.1. Evapotranspiration calculation using the water balance method

Although it is difficult to obtain evapotranspiration (ET) data for a watershed, accurate ET values can be estimated with water balance methods applied over sufficiently long time scales such as a full hydrological year. The water balance method proposed by Wisler and Brater (1959), which is shown in Eq. (1), was used to calculate the amount of ET of the simulated watershed in this study.

$$ET = P - r - \Delta S \quad (1)$$

where P is precipitation, r is runoff, and ΔS is the change in groundwater storage. Due to the lack of any surface runoff occurring in these simple watersheds, r + ΔS is the amount of groundwater recharge from precipitation. In this study, P is the total rain acquired from daily meteorological data at the Puding Karst Ecosystem Research Station; r is the runoff depth, i.e. the ratio of the spring discharge to the

simulated watershed area (20 m 5 m = 100 m^2), and ΔS is the water level change in the watersheds during the study period. Thus, according to Eq. (1), the ratio of ET to P can be determined from Eq. (2).

$$ET\% = (P - r - \Delta S)/P \quad (2)$$

3.2.2. Evaporation estimation using the $\delta D/\delta^{18}O$ (single isotope system) method

Stable hydrogen or oxygen isotopes have been widely used to separate evapotranspiration into the transpiration and evaporation components, as noted, because evaporation involves isotopic fractionation, but transpiration does not (Gibson et al., 1993; Yakir and Wang, 1996; Wang et al., 2013). Isotopic composition is expressed in terms of $^2H/^1H$ or $^{18}O/^{16}O$ ratios, represented by δ, such that $\delta = [(R_{sample}/R_{standard}) - 1] * 1000$, where $R = {}^2H/{}^1H$ or $^{18}O/^{16}O$ ratio in sample and standard (the standard is VSMOW). According to the isotope mass balance equations proposed by Gibson et al. (1993), the ratio of evaporation to precipitation (E) can be calculated using Eq. (3). Note that different E can be determined by either hydrogen or oxygen isotopic system, i.e. by δD or by $\delta^{18}O$; for convenience we term this the $\delta D/\delta^{18}O$ method.

$$E = ((\delta - \delta_0)(1 - h))/((\delta^* - \delta)h) \quad (3)$$

where δ is the mean isotopic composition of the groundwater, which could be δD or $\delta^{18}O$. δ_0 is the annual amount-weighted mean of the precipitation, and h is the mean relative humidity. δ^* is defined as

$$\delta^* = (h\delta_A + \varepsilon)/(h - \varepsilon) \quad (4)$$

where ε is the enrichment factor ($\varepsilon = \varepsilon^* + \varepsilon k$), which includes the equilibrium enrichment factor ($\varepsilon^* = 1000(\alpha^* - 1)$), dependent only on the temperature (T) (Eqs. (5) and (6)), and the kinetic enrichment factor (εk) associated with humidity and derived from Eqs. (7) and (8) (Craig and Gordon, 1965; Majoube, 1971; Gonfiantini, 1986; Clark and Fritz, 1997). δ_A is the mean isotopic composition of the water vapor, which is in equilibrium with the precipitation and is defined as $\delta_A = \delta_0 - \varepsilon^*$.

$$1000\ln\alpha * D = 24.844(10^6/T^2) - 76.248(10^3/T) + 52.612 \quad (5)$$

$$1000\ln\alpha * {}^{18}O = 1.137(10^6/T^2) - 0.4156(10^3/T) - 2.0667 \quad (6)$$

$$\varepsilon kD = 12.5(1 - h) \quad (7)$$

$$\varepsilon k^{18}O = 14.2(1 - h) \quad (8)$$

3.2.3. Evaporation estimation using the d-excess (dual isotope system) method

Compared to the $\delta D/\delta^{18}O$ method, which deals with the individual isotope systems, the d-excess method encompasses the dual isotope (D-^{18}O) system. Because the evaporation component evolves as described by the Rayleigh process (Clark and Fritz, 1997), it is assumed that groundwater evaporation in any watershed experiences Rayleigh fractionation, as shown in Eq. (9) where R represents the $^{18}O/^{16}O$ or $^2H/^1H$ ratio. For convenience, we use δ instead of R, so expressing the Rayleigh fractionation by δ (Eq. (10)). Thus, the relationship between d-excess and the residual fraction of groundwater (f) is derived as in Eq. (11). Here, 1 − f means the ratio of evaporation to precipitation.

$$R = R_0 f^{(\alpha - 1)} \quad (9)$$

$$\delta = (\delta_0 + 1000)f^{(\alpha - 1)} - 1000 \quad (10)$$

$$\begin{aligned} d &= \delta D - 8\delta^{18}O \\ &= (\delta D_0 + 1000)f^{(\alpha D - 1)} - 1000 - 8[(\delta^{18}O_0 + 1000)f^{(\alpha^{18}O - 1)} - 1000] \\ &= (\delta D_0 + 1000)f^{(\alpha D - 1)} - 8(\delta^{18}O_0 + 1000)f^{(\alpha^{18}O - 1)} + 7000 \end{aligned} \quad (11)$$

where α is the fractionation factor between the product and the reactant (note that it includes both the equilibrium and the kinetic fractionation factors) as shown in Eq. (12); α^* is the equilibrium fractionation factor derived from Eqs. (5) and (6); and the kinetic enrichment factor is obtained from Eqs. (7) and (8). In addition, $\delta^{18}O_0$ and δD_0 are the isotopic compositions of initial groundwater, which is the same as δ_0 in Eq. (3).

$$\alpha = \alpha_{product-reactant} = \alpha_{v-l} = 1/(\alpha^* + \varepsilon k/1000) \quad (12)$$

Therefore, the ratio of evaporation to precipitation (E = 1 − f) in the watershed can be calculated from Eq. (11).

3.2.4. Transpiration estimation

Based on E calculated using the d-excess or $\delta^{18}O/\delta D$ methods and on ET by the water balance method, the ratio of transpiration to precipitation (T) can be estimated (Eq. (13)), which is taken as the water loss to the atmosphere through plants, including interception.

$$T = ET - E \quad (13)$$

3.2.5. Groundwater residence time estimation

Groundwater residence times (MRT) in watersheds may be estimated by the seasonal variation relationships of $\delta^{18}O$ between precipitation and groundwater, assuming that the hydrologic system is well mixed and at a steady state in which the water residence time is presumed to approximate an exponential distribution (Stewart and McDonnell, 1991; Reddy et al., 2006). The seasonal variations of $\delta^{18}O$ tend to follow a sine functional relationship:

$$\delta^{18}O = I + A\sin[(2\pi t/b) + c] \quad (14)$$

where I is the annual mean $\delta^{18}O$ in ‰, A is the seasonal amplitude of $\delta^{18}O$, b is the period of the seasonal cycle, t is time in days, and c is the phase lag in radians. These parameters can be calculated by regression analysis, and groundwater MRT is obtained by Eq. (15) below:

$$MRT = (2\pi/b')[(A/A_p)^{-2} - 1]^{0.5} \quad (15)$$

where A_p is the seasonal amplitude of $\delta^{18}O$ of precipitation and b′ is the period of 365 days (Maloszewski et al., 1983).

4. RESULTS

4.1. Stable isotope composition of the precipitation and groundwater

The rainfall samples were used to determine the Local Meteoric Water Line (LMWL) for the study area (Fig. 2a). The best fit is $\delta D = 8.56\delta^{18}O + 17.14$ ($R^2 = 0.98$), which differs slightly from the Global Meteoric Water Line (GMWL) of Craig (1961). The isotopic composition of the ground waters are plotted in Fig. 2b, which shows that almost all of them plot to the right of the LMWL in the five simulated watersheds, indicating that the groundwater experienced evaporation.

The seasonal variations in the $\delta^{18}O$ of the precipitation and groundwater of the five simulated watersheds from November 2015 to November 2016 are shown in Fig. 3. $\delta^{18}O$ of the precipitation was heavier in the dry season than in the rainy season. In contrast, $\delta^{18}O$ values of ground waters were heavier in the rainy season than in the dry season. The gray dashed line in Fig. 3 represents the annual amount-weighted average $\delta^{18}O$ in the precipitation, which

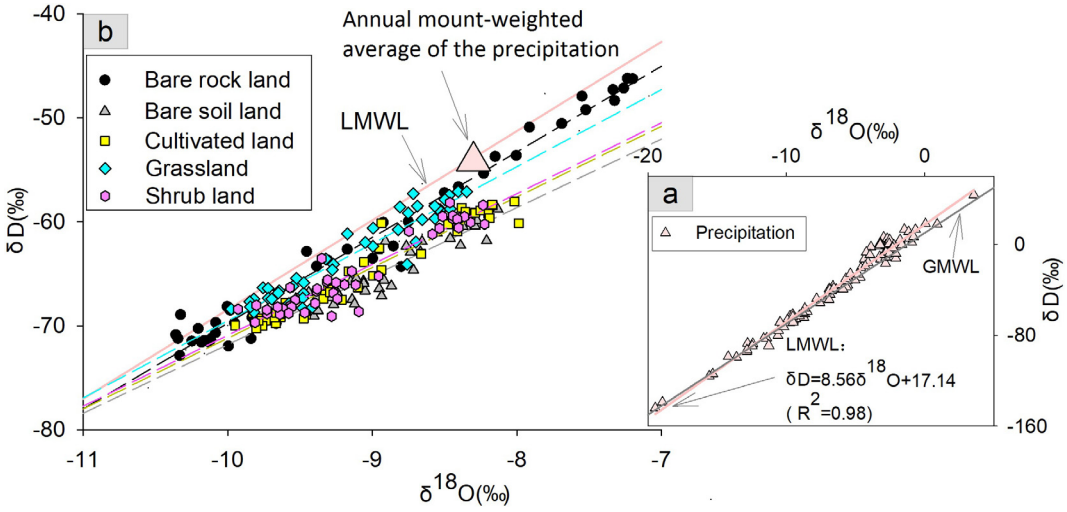

Fig. 2. (a) The stable isotope composition of the precipitation samples and (b) the relationships between the stable isotope composition of the groundwater samples and the LMWL (Local Meteoric Water Line). The dashed colored lines represent the evaporation lines of the groundwater: black for bare rock land ($\delta D = 8.25\delta^{18}O + 12.69$, $R^2 = 0.97$); gray for bare soil land ($\delta D = 6.59\delta^{18}O - 5.87$, $R^2 = 0.84$); dark yellow for cultivated land ($\delta D = 6.80\delta^{18}O - 3.20$, $R^2 = 0.94$); blue for grassland ($\delta D = 7.42\delta^{18}O + 4.66$, $R^2 = 0.89$); and pink for shrub land ($\delta D = 6.82\delta^{18}O - 2.73$, $R^2 = 0.89$). (For interpretation of the references to colour in this figure legend, the reader is referred to the web version of this article.)

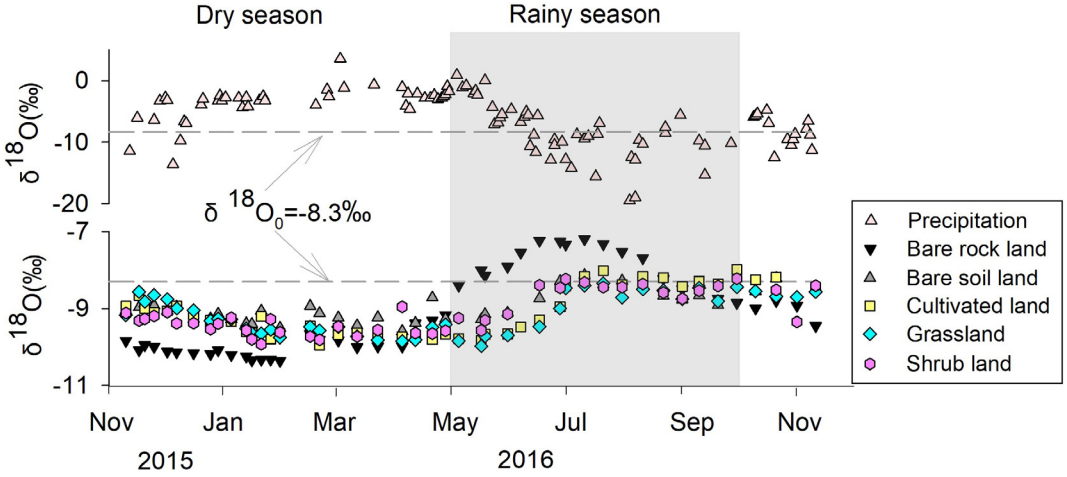

Fig. 3. Seasonal variations in the $\delta^{18}O$ of the precipitation and groundwater in the five simulated watersheds. The dashed gray lines represent the annual amount-weighted average of $\delta^{18}O$ in the precipitation (−8.3‰).

was −8.3‰. The $\delta^{18}O$ of the bare rock land had the largest fluctuation in response to $\delta^{18}O$ of the precipitation, while the $\delta^{18}O$ of the bare soil land was relatively smooth.

4.2. The d-excess of precipitation and groundwater

The seasonal variations in the d-excess in precipitation in the study area, November 2015 to November 2016, are shown in Fig. 4. Like $\delta^{18}O$, the value of d-excess varied regularly with time. It was high in the dry season and low in the rainy season, but appeared more stable than $\delta^{18}O$ during the rainy season. The probability distributions of $\delta^{18}O$ and d-excess during the rainy season are shown in Fig. 5. $\delta^{18}O$ values are quite widely dispersed, with the central range of −10‰ to −5‰ accounting for only 49% of the total rainfall during the rainy season. D-excess had a smaller range, 8–13‰ accounting for 71% of total rainy season precipitation.

The d-excess values of the groundwater in each of the five simulated watersheds are presented in Fig. 6. They do not display statistically significant seasonal variations and are relatively stable over the recorded hydrological year. Groundwater d-excess values follow the order: bare rock > grassland > shrub land > cultivated land > bare soil, distinguishing the groundwater under the different land uses. Furthermore, the d-excesses of groundwater were lower than the annual amount-weighted average and rainy season amount-weighted average in the precipitation.

4.3. Characteristics of groundwater recharge

4.3.1. Groundwater recharge rates

From the measured discharge and water level data, the recharge by precipitation was estimated based on water balances (Table 1), first for the hydrologic year and then for two different seasons. During the rainy season, recharge rates were 84.0% in bare rock land, 80.4% in bare soil land, 79.3% in cultivated land, 70.9% in grassland and 86.5% in shrub land, respectively, indicating that all five simulated watersheds were being recharged chiefly under the rainy season conditions, as expected.

4.3.2. Groundwater mean residence times

The groundwater MRT of the five simulated watersheds were calculated with Eq. (15) and are cited in Table 2. The MRT of groundwater was the shortest in the bare rock

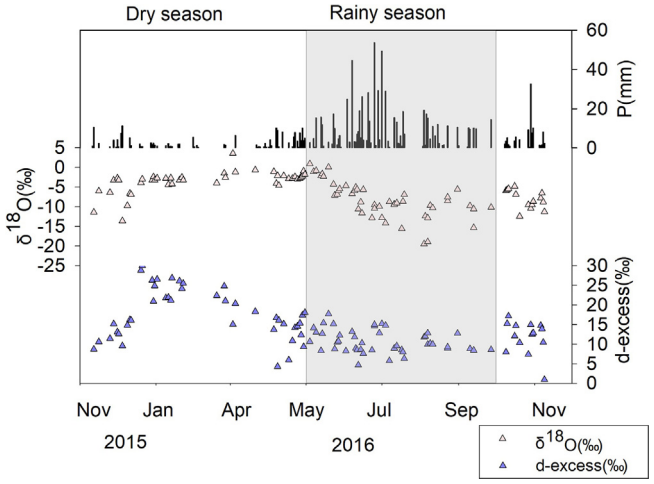

Fig. 4. Seasonal variations in the d-excess and $\delta^{18}O$ in precipitation at the Shawan Test Site.

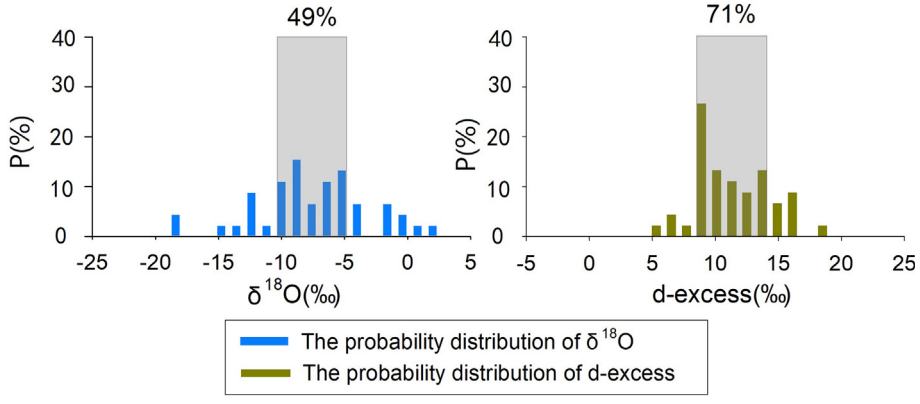

Fig. 5. The probability distribution of the $\delta^{18}O$ and d-excess in the precipitation samples in the rainy season.

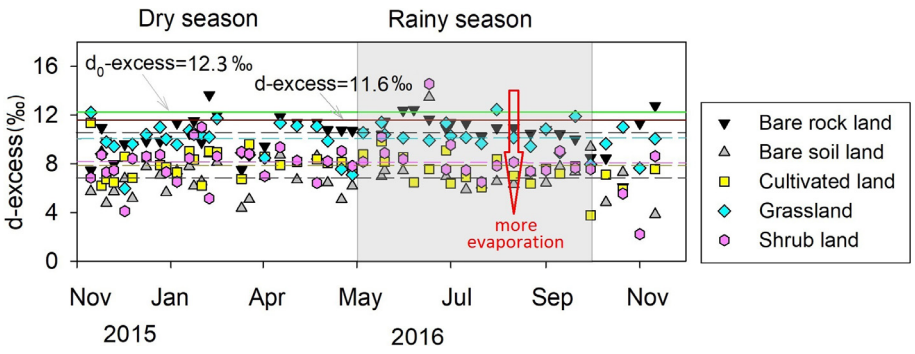

Fig. 6. Seasonal variations of the d-excess in groundwater from the five simulated watersheds. The solid lines represent the d-excess of initial groundwater: green is annual amount-weighted average of precipitation, and red is rainy season amount-weighted average of precipitation. The dashed colored lines represent the annual mean of d-excess in the ground waters: black for bare rock land (d-excess = 10.5‰); gray for bare soil land (d-excess = 6.8‰); dark yellow for cultivated land (d-excess = 7.8‰); blue for grassland (d-excess = 10.1‰); pink for shrub land (d-excess = 8.1‰). The results show that the d-excess decreases when there is more evaporation. (For interpretation of the references to colour in this figure legend, the reader is referred to the web version of this article.)

land, and the longest in the bare soil land. The durations were 191 days (0.52 years) in bare rock land, 509 days (1.39 years) in bare soil land, 261 days (0.71 years) in cultivated land, 381 days (1.04 years) in grassland and 349 days (0.95 years) in shrub land.

4.4. Calculation of the ET partition

4.4.1. Evaporation estimation using the $\delta D/\delta^{18}O$ and d-excess methods

$\delta D/\delta^{18}O$ and d-excess methods were applied to determine the amount of evaporation, based on the isotopic composition of the precipitation and groundwater over the recorded hydrological year. The average annual temperature and humidity, the initial isotopic composition of the groundwater (annual amount-weighted average of precipitation), and the isotopic composition of the groundwater are given in Table 3. We first calculated the amount of evaporation for the five simulated watersheds using the $\delta D/\delta^{18}O$ method (Eq. (3)), finding the results (Table 3) to be all negative, suggesting that these five simulated watersheds did not experience any evaporation at all! Using Eq. (11), the proportion of evaporation was calculated by the d-excess method. The relationship between the d-excess and the residual fraction of the groundwater (f) of the five watersheds is shown in Fig. 7. It suggests that the amounts of evaporation in these simulated watersheds were as follows: bare rock land < grassland < shrub land < cultivated land < bare soil land. The evaporation rates (1 − f) were 7.1% for bare rock land, 9.0% for grassland, 16.6% for shrub land, 17.7% for cultivated land, and 21.4% for bare soil land (Table 3).

4.4.2. Transpiration estimation

The ET in the five simulated watersheds was calculated first, applying Eq. (2). The results (Table 4) were: 5.9% for the bare rock land, 36.2% for the bare soil land, 40.6% for the cultivated land, 64.1% for the grassland, and 57.2% for the shrub land. Based on the evapotranspiration data derived from the water balances and the evaporation from the d-excess, transpiration was calculated as reported in Table 4. There were no plants in the bare rock and bare soil lands, so their transpiration was 0%. The transpiration rates were 23.3% for the cultivated land, 55.0% for the grassland, and 40.4% for the shrub land. Thus, the ratios of transpiration to evapotranspiration were 56.8% for the cultivated land, 85.9% for the grassland, and 70.9% for the shrub land.

5. DISCUSSION

5.1. Groundwater is affected by evaporation in the simulated watersheds

As a result of isotopic kinetic fractionation, residual water after evaporation will display trends similar to the LMWL but with lower slopes in the $\delta^{18}O$-δD plots (Clark and Fritz, 1997; Schulte et al., 2011). The isotopic compositions of the groundwater in the five simulated watersheds almost all plot to the right of the LMWL (Fig. 2b), indicating that the groundwater has been affected by evaporation. This conclusion is corroborated by the d-excess of groundwater plotted in Fig. 6 because d-excesses of ground waters differed under different land uses and was lower than their initial d-excesses (annual amount-weighted average or rainy season amount-weighted average of precipitation) because the d-excess decreased when evaporation increased. As a result, the degree of evaporation is: bare soil land > cultivated land > shrub land > grassland > bare rock land.

5.2. The $\delta^{18}O$ and d-excess of precipitation and groundwater

5.2.1. Seasonal variations of $\delta^{18}O$ and d-excess of precipitation

Due to the linear relationship between δD and $\delta^{18}O$ ($\delta D = 8.56\delta^{18}O + 17.14$) in the precipitation, we do not discuss the variability of δD in this paper. Seasonal variations in $\delta^{18}O$ and d-excess in the precipitation were high in the dry season and low in the rainy season (Fig. 4), which was mainly due to the differences in the water vapor sources and is consistent with the findings of other precipitation studies in Southwestern China, e.g. Zhang et al. (2008).

Table 1
Groundwater recharge rates in the five different simulated watersheds.

ID	One year (2015/11–2016/10)			Dry season (2015/11–2016/04)			Rainy season (2016/05–2016/10)			
	Runoff depth (m/a)	ΔH[a] (m)	Recharge[b] (m/a)	Runoff depth (m/a)	ΔH[a] (m)	Recharge[b] (m/a)	Recharge rate[c] (%)	Runoff Depth (m/a)	ΔH[a] (m)	Recharge[b] (m/a)	Recharge rate[c] (%)
Bare rock land	1.137	−0.421	0.927	0.593	−0.890	0.148	16.0	0.544	0.470	0.779	84.0
Bare soil land	0.838	−0.420	0.628	0.433	−0.620	0.123	19.6	0.405	0.200	0.505	80.4
Cultivated land	0.800	−0.429	0.585	0.429	−0.615	0.121	20.7	0.371	0.185	0.464	79.3
Grassland	0.534	−0.360	0.354	0.334	−0.462	0.103	29.1	0.200	0.102	0.256	70.9
Shrub land	0.632	−0.420	0.422	0.332	−0.550	0.057	13.5	0.300	0.130	0.365	86.5

[a] ΔH is the water level change.
[b] Recharge is the amount of groundwater supplied by precipitation, and Recharge = ΔS + Runoff depth, where ΔS = ΔH * Porosity.
[c] Recharge rate during a selected period is the recharge in that time divided by the total recharge. For example, the recharge rate during dry season is the recharge of dry season divided by the recharge of the one hydrological year.

Because the study site has a subtropical monsoon climate, the water vapor comes mainly from the low latitude ocean in the rainy season, resulting in very high humidity that readily creates strongly convective weather with much precipitation along its path, resulting in significant rainout effect, depleted $\delta^{18}O$ and lower d-excess. In contrast, the main source of water vapor in the dry season is the cold, dry continental air mass of Siberia and inland recycled water vapor, which results in less precipitation, more enriched $\delta^{18}O$, and higher d-excess.

5.2.2. The stability of the d-excess of precipitation compared to the $\delta^{18}O$ in the rainy season

Precipitation, especially frequent heavy rainfall, occurs mainly in the rainy season from May to October, as noted, and accounts for more than 80% of mean annual rainfall. The groundwater of the five simulated watersheds was primarily recharged by rainy season precipitation (Table 1). As a result, the input characteristics of the groundwater were dominated by the rainy season precipitation; it is important to study characteristics of that precipitation. The variations and probability distributions of $\delta^{18}O$ and d-excess during the rainy season (Figs. 4 and 5), indicate that the d-excess was much more stable than the $\delta^{18}O$. The same conclusion can be reached in Xie et al. (2011) who studied the δD and $\delta^{18}O$ of precipitation in Guangzhou over three years.

Why is d-excess more stable than $\delta^{18}O$ in precipitation? The evolution of d-excess and $\delta^{18}O$ through a full hydrologic cycle, based on isotopic theoretical analysis, begins with the evaporation of seawater to atmospheric vapor; then, atmospheric vapor condenses into precipitation, the groundwater is recharged, followed by evaporation (Fig. 8). The evaporation model proposed by Craig and Gordon (1965) demonstrates that water vapor in the immediate vicinity of a water surface is in isotopic equilibrium with that water. Thus seawater forms an initial equilibrium vapor with a slope ($s = (\delta D - \delta D_0)/(\delta^{18}O - \delta^{18}O_0) = (\alpha_{v\text{-}l}D - 1)/(\alpha^{18}_{v\text{-}l}O - 1)$), Clark and Fritz, 1997) of 8, which takes the slope of GMWL as reference, resulting in the value of d-excess remaining unchanged. However, the temperature will affect the d-excess value (Gat, 1996; Luz and Barkan, 2010), and the d-excess of the equilibrium vapor is more positive when the surface temperature of the seawater is higher (Fig. 8). Then the equilibrium vapor diffuses into the free air above due to the presence of a vapor concentration gradient, leading to kinetic fractionation that results in slopes less than 8. Kinetic diffusion fractionation increases the d-excess value of the vapor, the amount of increase depending on the moisture gradient, i.e., the d-excess of the vapor will increase when the gradient becomes steeper due to lower humidity in the air (Fig. 8).

The atmospheric vapor formed by these processes condenses into precipitation under isotopic equilibrium, as in the model of Craig and Gordon (1965). Similarly, the condensation temperature influences the d-excess of the precipitation. As seen in Fig. 8, when the atmospheric vapor condenses into droplets, δD and $\delta^{18}O$ change along the Global (or Local) meteoric water line, accompanied by the effects of rainout, but the d-excess of the precipitation

Table 2
Summary of results for fitting the sine function to the seasonal variations of $\delta^{18}O$ in precipitation and groundwater, and the estimated groundwater MRTs in the five different simulated watersheds.

ID	I(‰)	A(‰)	b	c(rad)	R^{2}[a]	A/A_P	MRT [days (years)]
Precipitation	−6.2	4.4	464	−6.28	0.52	NA[b]	NA[b]
Bare rock land	−9.3	1.3	534	−6.28	0.78	0.29	190 (0.52)
Bare soil land	−8.8	0.5	602	−6.28	0.64	0.11	509 (1.39)
Cultivated land	−8.7	1.0	546	−6.28	0.79	0.22	261 (0.71)
Grassland	−9.2	0.7	295	−6.28	0.69	0.15	381 (1.04)
Shrub land	−8.8	0.7	587	−6.28	0.77	0.16	349 (0.95)

Note: Seasonal variations of $\delta^{18}O$ follow a sine function equation:
$\delta^{18}O = I + A\sin[(2\pi t/b) + c]$ (14)
where I is the annual mean $\delta^{18}O$ in ‰, A is the seasonal amplitude of $\delta^{18}O$, b is the period of the seasonal cycle, t is time in days, and c is the phase lag in radians. These parameters can be calculated by regression analysis, and groundwater MRT is obtained by the Eq. (15) below:
$MRT = (2\pi/b')[(A/A_p)^{-2} - 1]^{0.5}$ (15)
where A_p is the seasonal amplitude of $\delta^{18}O$ in precipitation and b′ is the period of 365 days (Maloszewski et al., 1983).
[a] Rsqr of the regression line for each watershed.
[b] Not applicable.

Table 3
δD, $\delta^{18}O$ and d-excess of groundwater, and the estimated evaporation rate (E).

ID	t (°C)[a]	h (%)[a]	δD_0 (‰)[b]	$\delta^{18}O_0$ (‰)[b]	d_0-excess (‰)[b]	δD (‰)[b]	$\delta^{18}O$ (‰)[b]	d-excess (‰)[b]	E (%)		
									δD method[c]	$\delta^{18}O$ method[c]	d-excess method[d]
Bare rock land	15.1	78	−54.2	−8.3	12.3	−62.6	−9.1	10.5	−3.8	−2.6	7.1
Bare soil land						−64.9	−9.0	6.8	−4.7	−2.1	21.4
Cultivated land						−65.0	−9.1	7.8	−4.7	−2.5	17.7
Grassland						−63.1	−9.2	10.1	−4.0	−2.6	9.0
Shrub land						−64.9	−9.1	8.1	−4.7	−2.5	16.6

[a] t(°C) and h(%) are annual average temperature and relative humidity, respectively.
[b] $\delta^{18}O_0$ (or δD_0) and d_0-excess are the isotopic compositions of the initial groundwater, which is the annual amount-weighted average of the precipitation, and the $\delta^{18}O$ (or δD) and d-excess are the mean isotopic compositions of the groundwater for the full hydrological year.
[c] The ratio of evapotranspiration to precipitation (E) is calculated using the $\delta D/\delta^{18}O$ method (Eq. (3)).
[d] The ratio of evapotranspiration to precipitation (E) is derived from the d-excess method (Eq. (11)).

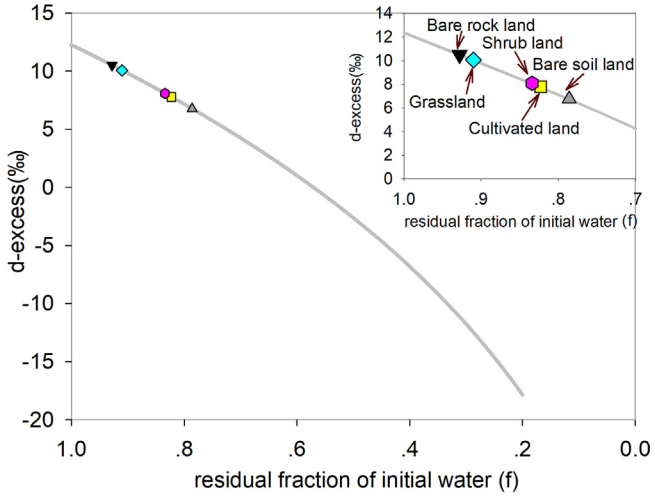

Fig. 7. The relationship between d-excess and the residual fraction of groundwater for the five different land use watersheds at the test site.

Table 4
Calculated transpiration for the five different simulated watersheds.

ID	Water balance method						d-excess method		
	Precipitation (P, m/a)	Porosity[a]	ΔH[b] (m)	Runoff depth (r, m/a)	Infiltration coefficient (%)[c]	ET(%)[c]	E(%)	T(%)[d]	T/ET (%)
Bare rock land			−0.421	1.137	94.1	5.9	7.1	0	0
Bare soil land			−0.420	0.838	63.8	36.2	21.4	0	0
Cultivated land	0.985	0.5	−0.429	0.800	59.4	40.6	17.7	23.3	56.8
Grassland			−0.360	0.534	35.9	64.1	9.0	55.0	85.9
Shrub land			−0.420	0.632	42.8	57.2	16.6	40.4	70.9

Note: The duration of the study was from November 2015 to October 2016, covering a full hydrological year.
[a] The porosity value is from Zhu et al. (2015). It was the same for the five different simulated watersheds (Zhu et al., 2015).
[b] ΔH is the water level change.
[c] ET is the ratio of evapotranspiration to precipitation, which can be calculated by using Eq. (2): ET% = (P-r-ΔS)/P, where ΔS = ΔH * Porosity. Infiltration coefficient = 1 − ET.
[d] T is the ratio of transpiration to precipitation, estimated by T = ET–E based on Eq. (13).

remains at some given value; as a result, the δD and $\delta^{18}O$ of precipitation are considerably more variable than the d-excess. For example, the δD and $\delta^{18}O$ in precipitation associated with typhoons are lower than those of normal summer precipitation, but their d-excess values are almost identical (Xie et al., 2011). Because the primary vapor source during the rainy season is from low latitude ocean with high humidity, different precipitation events have the same vapor source, so identical original environmental factors influence d-excess, δD and $\delta^{18}O$ in different precipitation events within a given area: the d-excess remains at approximately the same value in different precipitation events, and the considerable variations of δD and $\delta^{18}O$ are caused by the rainout effects. According to the model of d-excess variation shown in Fig. 8, d-excess in precipitation will increase when the vapor source comes from the recirculated vapor of a local water body, e.g., a lake (Machavaram and Krishnamurthy, 1995; Vallet-Coulomb et al., 2008). In our study, there were a few rainy season precipitation d-excess values as high as 17.7‰ (Fig. 4), which were very likely caused by recirculated vapor from Yelang Lake a few km from the study area (Fig. 1a).

5.2.3. Seasonal variations of $\delta^{18}O$ and d-excess of groundwater

The $\delta^{18}O$ of groundwater in the five simulated watersheds showed obvious seasonal variations (Fig. 3), whereas the d-excess of groundwater in the studied watersheds did

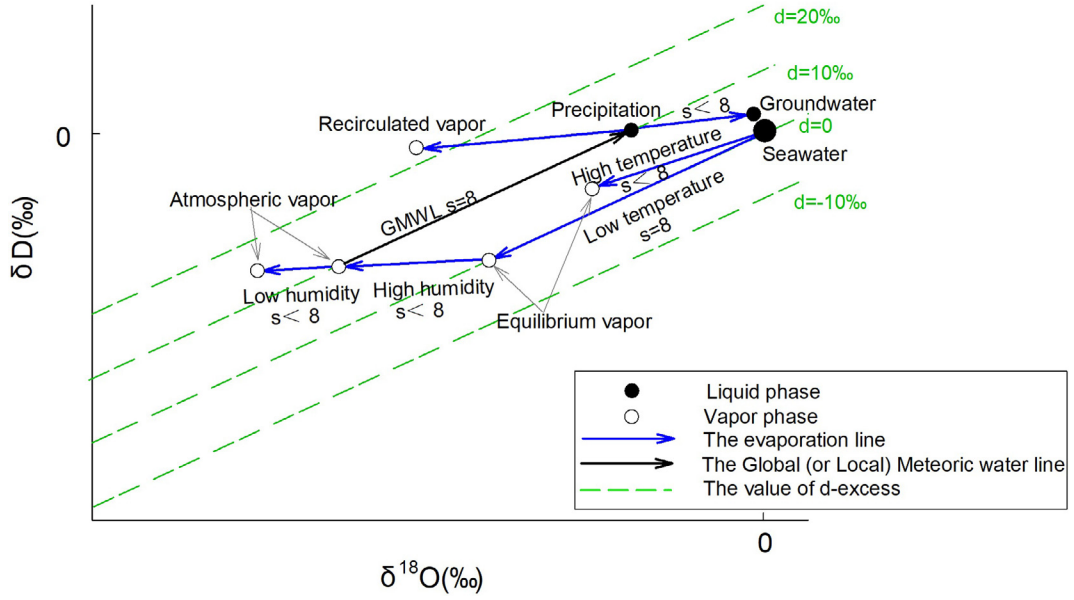

Fig. 8. Schematic showing variations in d-excess, $\delta^{18}O$ and δD over a full hydrologic cycle, which begins with the evaporation of seawater to form (i) sea surface equilibrium vapor, which diffuses upwards to form (ii) atmospheric vapor; (iii) the atmospheric vapor condenses into precipitation; (iv) groundwater recharge, with (v) the likelihood of evaporation. s represents the slope in the $\delta^{18}O$-δD plot. According to Clark and Fritz (1997), the relationship can be defined as $s = (\delta D - \delta D_0)/(\delta^{18}O - \delta^{18}O_0) = (\alpha_{v\text{-}l}D - 1)/(\alpha^{18}_{v\text{-}l}O - 1)$.

not, their values remaining relatively constant throughout the hydrological year (Fig. 6). Based on the characteristics of $\delta^{18}O$ and d-excess of precipitation, the stability of the d-excess of the ground waters was probably due to the stability of d-excess in the rainy season precipitation, while the groundwater seasonal variations of $\delta^{18}O$ reflect the substantial variations in $\delta^{18}O$ in rainy season precipitation.

For the estimation of evaporation, a stable index for the input signal that satisfactorily reflects the degree of prior evaporation will have a large impact on the accurate quantification of the evaporation in watersheds. However, many studies have been based only upon δD and $\delta^{18}O$, parameters that may vary greatly with precipitation.

5.3. Separating evapotranspiration into the evaporation and transpiration components

5.3.1. Evaporation estimation using the $\delta D/\delta^{18}O$ and d-excess method

Using the $\delta D/\delta^{18}O$ method, the evaporation in the five simulated watersheds was found to be negative (Table 3) because the δD_0 and $\delta^{18}O_0$ of the initial water (annual amount-weighted average of precipitation) were higher than the δD and $\delta^{18}O$ of the groundwater ($\delta < \delta_0$). Thus, the $\delta D/\delta^{18}O$ method failed to calculate acceptable evaporation values for the watersheds in this study.

The relationship between the d-excesses and the residual fractions of the groundwater (f) in the simulated watersheds in this experiment are plotted in Fig. 7. It shows that d-excess decreases with the decreasing residual fraction of the initial water when evaporation occurs. The d-excess and f of the groundwater in the simulated watersheds evolved along the same theoretical d-excess-f curve because the meteorological factors were the same for all of them. From Figs. 6 and 7 and Table 3, we conclude that the amounts of evaporation in the five tanks were as follows: bare rock < grassland < shrub land < cultivated land < bare soil. Land use patterns play a significant role in controlling evaporation. In the bare rock tank, the surface was coarsely granular with large pore spaces and no soil or plants to intercept the rain, which quickly and directly recharged the groundwater reservoir, resulting in comparatively rapid through-flow and the shortest MRT (Table 2); evaporation losses were very limited. The low evaporation rate in the grassland was caused by the large leaf area index of the alfalfa, which resulted in almost no bare soil being exposed to the air and protected the soil from much evaporation. Soil was more exposed in the shrub land and cultivated land due to their lesser leaf areas, so evaporation was stronger than in the grassland. Evaporation was largest on the bare soil land because of lack of protective plant cover and the fine-grained, water-retentive nature of the soil. In addition, there were no plants in the bare rock and bare soil lands, so the evapotranspiration calculated using the water balance method was from evaporation alone. The results agreed well with those obtained using the d-excess method, showing good consistency for the bare rock land (5.9% vs 7.1%), but were less consistent for the bare soil land (36.2% vs 21.4%, Table 4). The difference for the bare soil land was probably due to the strong evaporation, which resulted in low groundwater recharge rates and longer groundwater MRT (Table 2). Thus, the d-excess of the groundwater in the bare soil land was the integrated signature of a lengthy MRT, which made the evapotranspiration for bare soil land close to the average for approximately 1.39 years, and a low evaporation loss of only 28% for the 2014 dry season (as determined by Zhu et al., 2015). This implies that the relatively low evaporation rates calculated by the d-excess method, were influenced by low evaporation rates in the previous year. In contrast, the residence time of groundwater in the bare rock land was relatively short, so it aligned with the result calculated by the water balance method.

The reason why we failed to use the $\delta D/\delta^{18}O$ method was $\delta < \delta_0$. Why were the δD_0 and $\delta^{18}O_0$ values higher than the δD and $\delta^{18}O$ of the groundwater? When we compare seasonal variations in the $\delta^{18}O$ of the precipitation and the groundwater in the simulated watersheds (Fig. 3), we find a significant time lag (more than 0.5 year, Table 2) between the precipitation and the groundwater. Unlike the precipitation, groundwater $\delta^{18}O$ was heavier in the rainy season than in the dry season, which may indicate that the groundwater flows in a diffuse mode, with the result that there is mixing of waters of different ages in the simulated watersheds. The lighter $\delta^{18}O$ of the groundwater in the dry season was probably due to heavier rains in the previous year (1635 mm in 2015, compared to 963 mm in 2016), whereas the groundwater d-excess was relatively stable (Fig. 6) because it inherited the d-excess stability of rainy season precipitation. Therefore, given the strong variability of δD and $\delta^{18}O$ in the initial input signal of the groundwater, evaporation calculated by the $\delta D/\delta^{18}O$ method is sensitive to groundwater MRT and may be problematic when we quantify the evaporation flux at the watershed scale. The d-excess method is more suitable for studying evaporation and quantifying the hydrologic cycle in a watershed, especially in the East Asian monsoon region with changeable $\delta^{18}O$ and δD values but stable d-excess.

5.3.2. Transpiration and the ratio of transpiration to evapotranspiration

From the evapotranspiration estimates obtained by the water balance method and the evaporation results from the d-excess method, net transpiration can be derived (Table 4), yielding the ratios of transpiration to evapotranspiration in the simulated watersheds. The ratios were 56.8% for the cultivated land, 85.9% for the grassland, and 70.9% for the shrub land, demonstrating that the flux of water from vegetated watersheds to the atmosphere is mainly controlled by plant transpiration. Given this predominance, future water management in watersheds should pay more attention to the role of plant transpiration. Furthermore, the transpiration is closely linked to carbon assimilation by vegetation owing to the relationship between the water and carbon cycles (Nobel, 1999; Beer et al., 2007). Therefore, separating evapotranspiration into evaporation and transpiration components in watersheds is also essential for studying the carbon cycle.

6. CONCLUSIONS

(1) The isotopic compositions of the ground waters in the five simulated watersheds almost all plot to the right of the LMWL, indicating that the groundwater was affected by evaporation. Evaporation can also be reflected by d-excess, i.e., the d-excess decreases when there is more evaporation.
(2) The groundwater recharge was mostly derived from the rainy season precipitation, which averages for more than 80% of the total annual rainfall. In the rainy season, the $\delta^{18}O$ of precipitation is very variable, but the d-excess has a smaller range, resulting in significant variability of $\delta^{18}O$ but stability of d-excess in the groundwater. Therefore, in the rainy season, when most of the groundwater recharge occurs, the d-excess of precipitation is much more stable than $\delta^{18}O$, indicating that d-excess method is more suitable for estimating evaporation than the $\delta D/\delta^{18}O$ method.
(3) The evaporation rates calculated based on the d-excess method in the five simulated watersheds were 7.1% for bare rock land, 9.0% for grassland, 16.6% for shrub land, 17.7% for cultivated land, and 21.4% for bare soil land.
(4) Based on the water balance method, the ratio of evapotranspiration to precipitation was 5.9% on the bare rock land, 36.2% on the bare soil land, 40.6% on the cultivated land, 64.1% on the grassland, and 57.2% on the shrub land. Based on the evapotranspiration and evaporation data, the transpiration rates were found to be 0% for the bare rock land and bare soil land, 23.3% for the cultivated land, 55.0% for the grassland, and 40.4% for the shrub land. Therefore, the ratios of transpiration to evapotranspiration were 56.8% for the cultivated land, 85.9% for the grassland, and 70.9% for the shrub land, indicating that their watershed water cycle were controlled chiefly by plant transpiration.

ACKNOWLEDGEMENTS

This work was supported by the National Natural Science Foundation of China (U1612441, 41430753, 41673136). Special thanks are given to Prof. Dr. Derek Ford (McMaster University, Canada) for his thoughtful comments and corrections, which greatly improved the original draft.

REFERENCES

Araguas-Araguas L., Froehlich K. and Rozanski K. (1998) Stable isotope composition of precipitation over southeast Asia. *J. Geophys. Res.* **103**, 28721–28742.
Beer C., Reichstein M., Ciais P., Farquhar G. D. and Papale D. (2007) Mean annual GPP of Europe derived from its water balance. *Geophys. Res. Lett.* **34**, L05401.
Chen B., Yang R., Liu Z. H., Sun H. L., Yan H., Zeng Q. R., Zeng S. B., Zeng C. and Zhao M. (2017) Coupled control of land uses and aquatic biological processes on the diurnal hydrochemical variations in the five ponds at the Shawan Karst Test Site, China: implications for the carbonate weathering-related carbon sink. *Chem. Geol.* **456**, 58–71.
Clark I. D. and Fritz P. (1997) *Environmental Isotopes in Hydrogeology*. Lewis, Boca Ration.
Craig H. (1961) Isotopic variations in meteoric waters. *Science* **133**, 1702–1703.
Craig H. and Gordon L. I. (1965) Deuterium and oxygen-18 variation in the ocean and the marine atmosphere. In Stable Isotope in Oceanographic Studies and Paleotemperatures (eds. E. Tongiorgi). pp. 9–122.
Dansgaard W. (1964) Stable isotopes in precipitation. *Tellus* **16**, 436–468.
Ehleringer J. and Dawson T. (1992) Water uptake by plants: perspectives from stable isotope composition. *Plant Cell Environ.* **15**, 1073–1082.
Ferguson P. R. and Veizer J. (2007) Coupling of water and carbon fluxes via the terrestrial biosphere and its significance to the Earth's climate system. *J. Geophys. Res.* **112**, D24S06.
Gat J. R. (1996) Oxygen and hydrogen isotopes in the hydrologic cycle. *Annu. Rev. Earth Planet. Sci.* **24**, 225–262.
Gibson J. J., Edwards T. W. D. and Bursey G. G. (1993) Estimating evaporation using stable isotopes: quantitative results and sensitivity analysis for two catchments in Northern Canada. *Nordic Hydrol.* **24**, 79–94.
Gonfiantini R. (1986) Environmental isotopes in lake studies. In Handbook of Environmental Isotope Geochemistry (eds. P. Fritz and J. C. Fontes). pp. 113–168.
Huang T. M. and Pang Z. H. (2012) The role of deuterium excess in determining the water salinisation mechanism: A case study of the arid Tarim River Basin, NW China. *Appl. Geochem.* **27**, 2382–2388.
Jasechko S., Sharp Z. D., Gibson J. J., Birks S. J., Yi Y. and Fawcett P. J. (2013) Terrestrial water fluxes dominated by transpiration. *Nature* **496**, 347–350.
Lee D. and Veizer J. (2003) Water and carbon cycles in the Mississippi River basin: potential implications for the Northern Hemisphere residual terrestrial sink. *Glob. Biogeochem. Cycles* **17**, 1–17.
Lis G., Wassenaar L. I. and Hendry M. J. (2008) High-precision laser spectroscopy D/H and $^{18}O/^{16}O$ measurements of microliter natural water samples. *Anal. Chem.* **80**, 287–293.
Liu Z. H., Dreybrodt W. and Wang H. (2010) A new direction in effective accounting for the atmospheric CO_2 budget: considering the combined action of carbonate dissolution, the global water cycle and photosynthetic uptake of DIC by aquatic organisms. *Earth-Sci. Rev.* **99**, 162–172.
Luz B. and Barkan E. (2010) Variations of $^{17}O/^{16}O$ and $^{18}O/^{16}O$ in meteoric waters. *Geochim. Cosmochim. Acta* **74**, 6276–6286.
Machavaram M. V. and Krishnamurthy R. V. (1995) Earth surface evaporative process: a case study from the Great Lakes region of the United States based on deuterium excess in precipitation. *Geochim. Cosmochim. Acta* **59**, 4279–4283.
Majoube M. (1971) Fractionation of oxygen-18 and deuterium in water vapor. *J. Chem. Phys.* **68**, 1423–1436.
Maloszewski P., Rauert W., Stichler W. and Hermann A. (1983) Application of flow models in an alpine catchment area using tritium and deuterium data. *J. Hydrol.* **66**, 319–330.
Masson-Delmotte V., Jouzel J., Landais A., Stievenard M., Johnsen S. J., White J. W. C., Werner M., Sveinbjornsdottir A. and Fuhrer K. (2005) GRIP deuterium excess reveals rapid and orbital-scale changes in Greenland moisture origin. *Science* **309**, 118–121.
Maxwell R. M. and Condon L. E. (2016) Connections between groundwater flow and transpiration partitioning. *Science* **353**, 377–380.

Nobel P. S. (1999) *Physicochemical and Environmental Plant Physiology*. Academic press, San Diego.

Reddy M. M., Schuster P., Kendall C. and Reddy M. B. (2006) Characterization of surface and ground water $\delta^{18}O$ seasonal variation and its use for estimating groundwater residence times. *Hydrol. Process.* **20**, 1753–1772.

Schlesinger W. H. and Jasechko S. (2014) Transpiration in the global water cycle. *Agri. Forest Meteorol.* **226–227**, 229–245.

Schulte P., Geldern R. V., Freitag H., Karim A., Négrel P., Petelet-Giraud E., Probst A., Probst J., Telmer K., Veizer J. and Barth J. A. C. (2011) Applications of stable water and carbon isotopes in watershed research: weathering, carbon cycling, and water balances. *Earth-Sci. Rev.* **109**, 20–31.

Stewart M. K. and McDonnell J. J. (1991) Modeling base flow soil water residence times from deuterium concentrations. *Water Resour. Res.* **27**, 2681–2693.

Sulman B. N., Roman D. T., Scanlon T. M., Wang L. X. and Novick K. A. (2016) Comparing methods for partitioning a decade of carbon dioxide and water vapor fluxes in a temperate forest. *Agri. For. Meteorol.* **189–190**, 115–117.

Sutanto S. J., van den Hurk B., Dirmeyer P. A., Seneviratne S. I., Röckmann T., Trenberth K. E., Blyth E. M., Wenninger J. and Hoffmann G. (2014) HESS Opinions "A perspective on isotope versus non-isotope approaches to determine the contribution of transpiration to total evaporation". *Hydrol. Earth Syst. Sci.* **18**, 2815–2827.

Telmer K. and Veizer J. (2000) Isotopic constraints on the transpiration, evaporation, energy, and gross primary production budgets of a large boreal watershed: Ottawa River Basin, Canada. *Glob. Biogeochem. Cycles* **14**, 149–165.

Vallet-Coulomb C., Gasse F. and Sonzogni C. (2008) Seasonal evolution of the isotopic composition of atmospheric water vapor above a tropical lake: deuterium excess and implication for water recycling. *Geochim. Cosmochim. Acta* **72**, 4661–4674.

Wang K. and Dickinson R. E. (2012) A review of global terrestrial evapotranspiration: observation, modeling, climatology, and climatic variability. *Rev. Geophys.* **50**, RG2005.

Wang L. X., Niu S. L., Good S. P., Soderberg K., McCabe M. F., Sherry R. A., Luo Y. Q., Zhou X. H., Xia J. Y. and Caylor K. K. (2013) The effect of warming on grassland evapotranspiration partitioning using laser-based isotope monitoring techniques. *Geochim. Cosmochim. Acta* **111**, 28–38.

Wershaw R. L., Friedman I., Heller S. J. and Frank P. A. (1966) Hydrogen isotopic fractionation of water passing through trees. In Advances in Organic Geochemistry (eds. G. D. Hobson and G. C. Speers). pp. 55–67.

Wisler C. O. and Brater E. F. (1959) *Hydrology*. John Wiley, New York.

Xie L. H., Wei G. J., Deng W. F. and Zhao X. L. (2011) Daily $\delta^{18}O$ and δD of precipitations from 2007 to 2009 in Guangzhou, South China: implications for changes of moisture sources. *J. Hydrol.* **400**, 477–489.

Yakir D. and Wang X. F. (1996) Fluxes of CO_2 and water between terrestrial vegetation and the atmosphere estimated from isotope measurements. *Nature* **380**, 515–517.

Yang R., Liu Z. H., Zeng C. and Zhao M. (2012) Response of epikarst hydrochemical changes to soil CO_2 and weather conditions at Chenqi, Puding, SW China. *J. Hydrol.* **468**, 151–158.

Zeng C. and Liu Z. H. (2013) Ideas of construction of simulation test field of karst water and carbon fluxes. *Resour. Environ. Engineer.* **27**, 196–200 (in Chinese with English abstract).

Zeng Q. R., Liu Z. H., Chen B., Hu Y. D., Zeng S. B., Zeng C., Yang R., He H. B., Zhu H., Cai X. L., Chen J. and Ou Y. (2017) Carbonate weathering-related carbon sink fluxes under different land uses: a case study from the Shawan Simulation Test Site, Puding, Southwest China. *Chem. Geol.* **474**, 63–80.

Zhang X. P., Liu J. M., Nakawo M. and Xie Z. C. (2008) Vapor origins revealed by deuterium excess in precipitation in Southwest China. *J. Glaciol. Geocryol.* **04**, 0613–0619 (In Chinese with English abstract).

Zhu H., Zeng C., Liu Z. H., Zeng Q. R. and Li L. L. (2015) Karst-related carbon sink flux variations caused by land use changes: an example from the Puding karst test site in Guizhou. *Hydrogeol. Engineer. Geol.* **42**, 120–125 (in Chinese with English abstract).

Associate editor: Sarah J. Feakins